Article

Discovery Medicine 2025; 37(200): 1974–1990
https://doi.org/10.24976/Discov.Med.202537200.170

HDAC1 Facilitates the Proliferation and Glycolysis in Diffuse Large B-Cell Lymphoma by Modulating PI3K/AKT/mTOR Pathway

Yanzheng Wang[1], Yan Wang[2], Shishu Wang[3], Furong Zhao[4], Xinmei Yuan[5], Xiujie Fan[6,*]

[1]Department of Medical Laboratory, Yantaishan Hospital, 264000 Yantai, Shandong, China
[2]Intensive Care Unit (ICU), Qingdao Central Hospital, University of Health and Rehabilitation Sciences (Qingdao Central Hospital), 266000 Qingdao, Shandong, China
[3]Department of Hematology, Qingdao Central Hospital, University of Health and Rehabilitation Sciences (Qingdao Central Hospital), 266000 Qingdao, Shandong, China
[4]Department of Pathology, Jinan Zhangqiu District People's Hospital, 250200 Jinan, Shandong, China
[5]Department of Blood Transfusion, Jinan Zhangqiu District People's Hospital, 250200 Jinan, Shandong, China
[6]Medical Laboratory Diagnosis Center, Jinan Central Hospital, 250013 Jinan, Shandong, China
*Correspondence: fanxiujiejn@163.com (Xiujie Fan)
Submitted: 20 June 2025 Revised: 12 August 2025 Accepted: 25 August 2025 Published: 20 September 2025

Background: Diffuse large B-cell lymphoma (DLBCL) is a type of highly heterogeneous malignancy. Histone deacetylase 1 (HDAC1) plays a key role in various malignancies, but its function remains elusive in DLBCL. This study aims to explore the pivotal role and the mechanism of HDAC1 in DLBCL.

Methods: HDAC1 expression was detected in DLBCL tissues and cells. The glycolytic activity was assessed using pyruvate, lactic acid and glucose consumption assay kits. Cell apoptosis and proliferative capacity were measured by flow cytometry, 3-(4,5)-dimethylthiahiazo (-z-y1)-3,5-di-phenytetrazoliumromide (MTT) and 5-Ethynyl-2′-deoxyuridine (EdU) assays. Western blotting was used to detect the expression of HDAC1, phosphatidylinositol 3-kinase/protein kinase B/mammalian target of rapamycin (PI3K/AKT/mTOR) and glycolysis-related proteins. The effects of HDAC1 on tumor growth *in vivo* were explored by establishing a xenotransplantation model. Expressions of HDAC1, Ki-67, and c-myc in mouse tumors were detected by means of immunohistochemistry.

Results: High levels of HDAC1 were found in DLBCL tissues and cells ($p < 0.05$). *HDAC1* knockdown repressed cell proliferation, glycolysis, and PI3K/AKT/mTOR pathway in DLBCL cells ($p < 0.05$). Moreover, 740Y-P (PI3K/AKT/mTOR pathway activator) partly reversed the inhibition of *HDAC1* knockdown on cell proliferation and glycolysis ($p < 0.05$). Importantly, tumor xenotransplantation models showed that *HDAC1* knockdown inhibited tumor growth *in vivo* ($p < 0.05$).

Conclusions: HDAC1 facilitates the proliferation and glycolysis of DLBCL by mediating the PI3K/AKT/mTOR pathway, offering a therapeutic target for DLBCL.

Keywords: HDAC1; glycolysis; proliferation; PI3K/AKT/mTOR; diffuse large B-cell lymphoma

Introduction

Diffuse large B-cell lymphoma (DLBCL) is a highly aggressive diffuse malignant proliferation disease of the lymphatic system, and exhibits extremely rapid growth and high malignancy [1,2]. DLBCL is classified into multiple subtypes, including germinal center B-cell (GCB) and activated B-cell (ABC), in view of their heterogeneity in etiology, genetics, histology, and clinical outcomes, which complicate both treatment and prognosis [3,4]. In-depth exploration of the molecular mechanism underlying the development of DLBCL can uncover therapeutic targets leading to potential gene-targeted therapies for this malignant disease.

A malignant tumor is an uncontrolled neoplasm characterized by abnormal cell proliferation, division, and differentiation under the action of a series of initiating and promoting factors [5,6]. Proliferation forms a crucial part of tumor progression. In normal cells, DNA replication, as well as cell division and death, are strictly regulated by genes, whereas cells in malignant tumors can proliferate uncontrollably when their proliferation capacity becomes unchecked. The undeterred proliferation of malignant cells arises from various factors, including oncogene activation, mutations in tumor suppressor genes, telomerase overexpression, and dysregulation of signaling pathways [7,8]. Other than this, abnormal energy metabolism is a core pathological characteristic of tumor cells [9]. Studies have shown that even under aerobic conditions, tumor

cells will prioritize glucose for aerobic glycolysis, in a phenomenon known as the Warburg effect that creates a favorable environment for tumor growth and proliferation [10,11]. Another study has confirmed that abnormal energy metabolism pathways in tumor cells can serve as therapeutic targets for tumors [12]. Therefore, it is important to elucidate the energy regulation mechanism and abnormal energy metabolism of tumor cells.

Histone deacetylase 1 (HDAC1) is an important member of the intracellular metalloproteinase family, which can regulate cell growth and apoptosis, as well as the transcription and expression of related genes [13]. According to several reports, HDAC1 is involved in the development of various tumors [14–16]. For instance, *HDAC1* silencing inhibited cell growth and promoted cell death in breast cancer [17]. Another study showed that HDAC1 expression was dramatically elevated in patients with ovarian cancer, positioning it as a potential diagnostic biomarker [18]. It has been found that increased HDAC1 expression in gastric cancer (GC) was related to tumor size and stage, lymph node metastasis, and differentiation degree [19]. Moreover, abnormal expression of HDAC1 was observed in lymphoma, and HDAC1 overexpression was related to poor prognosis [20]. Nevertheless, the role of HDAC1 in DLBCL progression, especially in proliferation and glycolysis, remains unclear.

Phosphatidylinositol 3-kinase/protein kinase B/mammalian target of rapamycin (PI3K/AKT/mTOR) pathway is the central regulator of physiological changes in human tumor cells and participates in various biological processes, including cell cycle, survival, epithelial-mesenchymal transition, substance metabolism, and angiogenesis [21]. By mediating the activation of p85 and p110, PI3K catalyzes the synthesis of phosphatidylinositol 4,5-bisphosphate into phosphatidylinositol 3,4,5-trisphosphate (PIP3) [22]. PIP3 regulates AKT and 3-phosphoinositide-dependent kinase 1 localization and activation. Activated AKT transmits signals to downstream factors, thereby affecting metabolism, proliferation, angiogenesis, and other processes of tumor cells [23]. Recent studies have demonstrated that activation of the PI3K/AKT pathway promotes tumor development and reprograms glucose metabolism by capitalizing on its anti-apoptosis and pro-proliferation effects [24,25]. HDAC1 also plays a promoting role in the glycolysis and progression of tumors [19,26]. HDAC1 promotes glioblastoma progression by stimulating the PI3K/AKT pathway [27]. The utilization of MS-275, a specific HDAC1 inhibitor, has been shown to suppress the malignant behavior and stemness of esophageal squamous cell carcinoma cells by inhibiting the PI3K/AKT/mTOR pathway [28]. However, whether HDAC1 plays a role in DLBCL cell proliferation and glycolysis by regulating PI3K/AKT/mTOR signaling remains to be elucidated.

In the present study, the effects of HDAC1 on the proliferative potential and glycolytic activities of DLBCL cells were preliminarily explored. Furthermore, to delineate its pivotal role in cellular dynamics, we explored whether HDAC1 regulates the PI3K/AKT/mTOR pathway in DLBCL.

Materials and Methods

Patient Specimens

Forty-six tumor specimens were obtained from patients diagnosed with DLBCL in Yantaishan Hospital from April 2024 to April 2025. All patients belong to the GCB subtypes. Inclusion criteria of this study are as follows: (1) patients diagnosed with DLBCL; (2) patients receiving first-time treatment, with no history of having received anti-tumor treatments such as chemotherapy or radiotherapy; (3) patients with complete pathological data; and (4) patients or their families who voluntarily signed the informed consent form. Patients with the following criteria were excluded: (1) patients with recurrent disease; (2) patients with primary mediastinal large B-cell lymphoma; (3) patients with other hematological disorders or other congenital immune disorders; (4) patients with other malignant tumors; (5) patients with severe functional failure of organs such as the heart, liver, lungs, and kidneys; (6) patients with mental disorders and cognitive dysfunction; and (7) women during lactation or pregnancy. In addition, lymphoid tissues were meticulously harvested from a cohort of 28 patients exhibiting reactive lymphoid hyperplasia during the same period, serving as a control for this study (normal group). The tissues obtained were preserved at –80 °C for subsequent experiments.

Bioinformatics Analysis

The Gene Expression Profiling and Interactive Analyses (GEPIA) database (http://gepia.cancer-pku.cn/) contains RNA sequences based on tumor and normal samples from The Cancer Genome Atlas (TCGA) and Genotype-Tissue Expression (GTEx) databases for the purpose of analyzing *HDAC1* expression in DLBCL tissues. *HDAC1* expression in DLBCL was searched in adherence to the following screening criteria: (1) Expression DIY: Boxplot; (2) Datasets Selection: DLBC; (3) Matched TCGA normal and GTEx data; (4) Other settings are the default settings of the online analysis tool. A total of 47 DLBCL tissues and 337 normal tissues fulfilling these conditions were found and gathered.

Cell Culture

Human DLBCL cell lines used in the current study were GCB-DLBCL subtype SU-DHL-8 (CL-0871, Pricella, Wuhan, China) and OCI-LY-7 (XY-H736, Xybio, Shanghai, China), along with human B-lymphoblastoid cell line GM12878 (YB-72035HC, Yu Bo, Shanghai, China). The cells were cultured in Iscove's modified Dulbecco's medium (IMDM, PM12206, PERFEMIKER, Shanghai,

China) supplemented with 10% fetal bovine serum (abs972, absin, Shanghai, China) and 1% penicillin/streptomycin (CSH9024, Chemstan, Wuhan, China). These cells were cultivated within an incubator at 37 °C and enriched with an atmosphere comprising 5% CO_2. All cell lines were subjected to rigorous short tandem repeat authentication and mycoplasma detection.

Transfection

Lentiviral vectors carrying *HDAC1* short-hairpin RNA (sh-*HDAC1*#1, sh-*HDAC1*#2, and sh-*HDAC1*#3) and non-targeted shRNA (sh-NC) sequences were provided by GenePharma (Shanghai, China). Lentiviruses were transfected into cells according to the manufacturer's instructions. After transfection, PI3K activator 740Y-P (20 µM, 1983, R&D, Minneapolis, MN, USA) was added for rescue experiments [29]. Cells were divided into control (OCI-LY-7 or SU-DHL-8 cells without any treatment), sh-NC, sh-*HDAC1*#1, sh-*HDAC1*#2, sh-*HDAC1*#3, sh-*HDAC1*#1+dimethyl sulfoxide (DMSO [the solvent of 740Y-P], 67-68-5, Sinopharm, Shanghai, China), and sh-*HDAC1*#1+740Y-P groups. Targeting sequences are listed as follows.

sh-NC:
Sense: 5′-GUAUGUUCCGGUAAGAUAUTT-3′;
Antisense: 5′-AUAUCUUACCGGAACAUACTT-3′.

sh-*HDAC1*#1:
Sense: 5′-CCCGGAGGAAAGUCUGUUATT-3′;
Antisense: 5′-UAACAGACUUUCCUCCGGGTG-3′.

sh-*HDAC1*#2:
Sense: 5′-GCUUCAAUCUAACUAUCAATT-3′;
Antisense: 5′-UUGAUAGUUAGAUUGAAGCAA-3′.

sh-*HDAC1*#3:
Sense: 5′-CGACUGUUUGAGAACCUUATT-3′;
Antisense: 5′-UAAGGUUCUCAAACAGUCGCT-3′.

Real-Time Quantitative Polymerase Chain Reaction (RT-qPCR)

Total RNA was isolated with TRIzol reagent (PM11648, PERFEMIKER, Shanghai, China), and reverse transcription of cDNA was performed with Transcript cDNA Synthesis kit (RP1100, Solarbio, Beijing, China). Amplification was conducted utilizing SYBR Green kit (SR1110, Solarbio, Beijing, China) with a PCR system (LightCycler 480, Roche, Basel, Switzerland). Relative expression of *HDAC1* was calculated using the $2^{-\Delta\Delta CT}$ method with glyceraldehyde-3-phosphate dehydrogenase (*GAPDH*) as endogenous control. Primer sequences are as follows:

HDAC1:
Forward: 5′-GCTGTGGTACTTGGTCATCT-3′;
Reverse: 5′-GAAT CCGCATGACTCATAAT-3′.
GAPDH:
Forward: 5′-GTCTCCTCTGACTTCAACAGCG-3′;
Reverse: 5′-ACCACCCTGTTGCTGTAGCCAA-3′.

3-(4,5)-dimethylthiahiazo (-z-y1)-3,5-di-phenytetrazoliumromide (MTT) Assay

The transfected cells were inoculated into a 96-well plate (2×10^3 cells/well). After the cells were incubated for 24, 48, 72, and 96 hours, 20 µL MTT reagent (M1020, Solarbio, Beijing, China) was added. Following a 4-hour incubation, absorbance at 490 nm was recorded with a microplate reader (ELx800, Bio-Tek, Windim, VT, USA).

Western Blotting

Protein was isolated by radioimmunoprecipitation assay buffering solution (P0013B, Beyotime, Shanghai, China). Bicinchoninic acid assay kit (P0010S, Beyotime, Shanghai, China) was utilized for identifying protein concentration. Equal amounts of proteins were separated by sodium dodecyl sulfate polyacrylamide gel electrophoresis and then transferred to polyvinylidene fluoride membranes (YA1701, Solarbio, Beijing, China). The membranes were blocked with 5% non-fat milk solution for 1 hour at 37 °C. Afterwards, the membranes were incubated with primary antibodies against HDAC1 (1:1000, ab109411, Abcam, Waltham, MA, USA), Glucose transporter type 1 (GLUT1, 1:1000, AF5462, Affinity, Cincinnati, OH, USA), Hexokinase 2 (HK2, 1:1000, DF6176, Affinity, Cincinnati, OH, USA), Pyruvate kinase isozyme M2 (PKM2, 1:1000, AF5234, Affinity, Cincinnati, OH, USA), Lactate dehydrogenase A (LDHA, 1:1000, DF6280, Affinity, Cincinnati, OH, USA), phosphorylated phosphoinositide 3-kinase (p-PI3K, 1:1000, phospho Tyr607, AF3241, Affinity, Cincinnati, OH, USA), PI3K (1:1000, AF6241, Affinity, Cincinnati, OH, USA), phosphorylated protein kinase B (p-AKT, 1:1000, phospho Ser473, 4060S, CST, Danvers, MA, USA), AKT (1:1000, 9272S, CST, Danvers, MA, USA), phosphorylated mammalian target of rapamycin (p-mTOR, 1:1000, phospho Ser2448, 2971S, CST, Danvers, MA, USA), mTOR (1:1000, 2972S, CST, Danvers, MA, USA), and GAPDH (1:3000, AF7021, Affinity, Cincinnati, OH, USA), followed by incubation with horseradish peroxidase (HRP)-conjugated secondary antibody (1:5000, S0001, Affinity, Cincinnati, OH, USA). The immunoreactions were visualized using an enhanced chemiluminescence (ECL) reagent (PE0010, Solarbio, Beijing, China) and observed under a luminescent image analyzer (5200, Tanon, Shanghai, China). Gray values were analyzed using the Quantity-One software (v4.4, Biorad laboratory, Hercules, CA, USA).

5-Ethynyl-2′-deoxyuridine (EdU) Staining

Logarithmic DLBCL cells were inoculated into 96-well plates with 4×10^5 cells/well. EdU (C0071S-1, Beyotime, Shanghai, China) was added to each well at a volume of 100 µL. After a 2-hour cultivation, cells were fixed with 4% paraformaldehyde (P0099, Beyotime, Shanghai, China) for 30 minutes. Then, the cells were meticulously stained with Hoechst 33342 reaction solution (C0071S-6, Beyotime, Shanghai, China) at ambient temperature for 30 minutes. Subsequently, images were photographed under microscopy (FV3000, Olympus, Tokyo, Japan). The EdU-positive cells were enumerated in terms of percentages using the following formula:

Percentage of EdU-positive cells (%) = (EdU-positive cells/Total number of cells) $\times$ 100.

Flow Cytometry

Cell apoptosis was detected through Annexin V-FITC/PI kit (C1383M, Beyotime, Shanghai, China). After resuspending with binding buffer, DLBCL cells (1×10^5) were stained using Annexin V-FITC/PI reagents in the dark. The apoptotic cells were analyzed by means of flow cytometry (FACScan, BD Biosciences, San Jose, CA, USA).

Glycolytic Analysis

The processed cells of each group were digested and centrifuged; subsequently, the supernatant was discarded, and the cell pellet was resuspended in an appropriate medium. The cell suspension was adjusted to a density of 1×10^5 cells/100 µL and then inoculated into 6-well plates. The plates were cultured in a 37 °C, 5% CO_2 incubator. After the cells adhered to the plate, the pyruvate assay kit (S0299S, Beyotime, Shanghai, China), lactic acid assay kit (S0208S, Beyotime, Shanghai, China), and glucose assay kit (BC2505, Solarbio, Beijing, China) were adopted to measure the production of pyruvate, lactic acid, and glucose consumption in DLBCL cells. The absorbance values of pyruvic acid, lactic acid, and glucose were detected at wavelengths of 570 nm, 450 nm, and 505 nm, respectively, using a microplate reader (BioTek Synergy, BioTek, Winooski, VT, USA), which can automatically determine the samples' corresponding concentrations. Taking the control group as the standard, the relative contents of pyruvate and lactic acid were expressed as the ratio of the experimental group to the control group. Using value in the control well containing only culture medium without cells as the initial glucose concentration, the concentration of glucose consumed was determined using the formula in following:

Concentration of glucose consumed = Initial glucose concentration – Measured glucose concentration.

Relative glucose consumption = Concentration of glucose consumed in the experimental group/Concentration of glucose consumed in the control group.

Xenograft Tumor Model

Ten BALB/c nude mice aged 4–6 weeks obtained from Shandong Aileke Biotechnology Co., Ltd. (SCXK (Lu) 2022 0001) were randomly divided into two groups, with five mice in each group. The mice were subcutaneously administered with sh-NC and sh-*HDAC1*#1 OCI-LY-7 cells (1×10^4), respectively. All the mice were raised in a specific pathogen-free environment, with the room temperature set at 25 °C and the humidity at 70%. The tumor formation rate was observed 7 days after injection (tumor modeling was considered successful if the tumor had grown to a volume of 3 to 4 mm^3). All the nude mice in both groups developed tumors subcutaneously. After 28 days, the mice were sacrificed through CO_2 inhalation. Tumors were removed for measurements of volume, weighing, sectioning and immunohistochemical analysis. The tumor volume was determined using the following formula:

Volume = 0.5 $\times$ Length $\times$ $Width^2$.

Immunohistochemical Analysis

Tissue sections were dewaxed and dehydrated in xylene and a gradient of ethanol solutions, respectively. Subsequently, the sections were subjected to heating at an elevated temperature of 98 °C for 15 minutes in a 0.01 M citrate buffer, followed by the application of 3% hydrogen peroxide for an additional period of 10 minutes. After a 30-minute incubation with normal serum, the tissue sections were successively incubated with primary antibody against HDAC1 (1:100, ab109411, Abcam, Waltham, MA, USA), Ki67 (1:200, AF0198, Affinity, Cincinnati, OH, USA), c-myc (1:500, ab32072, Abcam, Waltham, MA, USA), followed by incubation with secondary antibody (1:200, S0001, Affinity, Cincinnati, OH, USA). After staining with 3, 3′-diaminobenzidine (P0202, Beyotime, Shanghai, China), the sections were evaluated under a microscope (DM3000, Leica, Wetzlar, Germany).

Statistical Analysis

GraphPad Prism software (v8.0, GraphPad Software, Inc., San Diego, CA, USA) was adopted for data processing. All data are presented as mean $\pm$ standard deviation. To compare two groups, the Student's *t*-test was utilized, whereas the analysis of variance (ANOVA) followed by Tukey's test was employed for comparisons involving multiple groups. A $p < 0.05$ was defined as statistically significant.

Results

HDAC1 was Elevated in DLBCL

HDAC1 expression in 46 DLBCL and 28 reactive lymphoid hyperplasia was examined using RT-qPCR. *HDAC1* expression was increased in DLBCL tissues versus normal tissues (Fig. 1a) ($p < 0.05$). Meanwhile, bioinformatics analysis demonstrated that *HDAC1* expression was

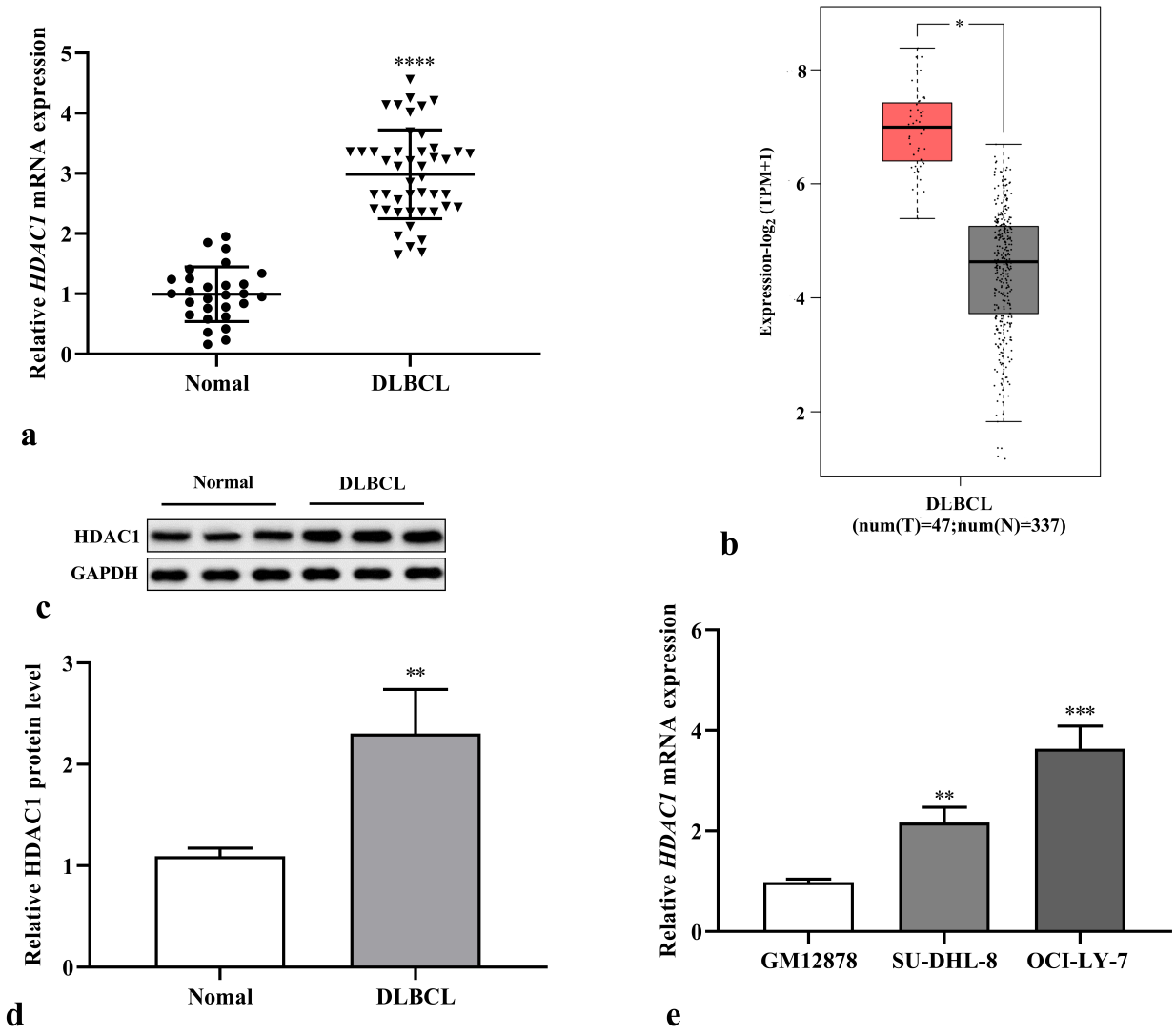

Fig. 1. HDAC1 was up-regulated in DLBCL. (a) *HDAC1* expression in 46 DLBCL samples and 28 reactive lymphoid hyperplasia samples was assessed by means of RT-qPCR (normal: $n = 28$; DLBCL: $n = 46$). (b) TCGA data from the GEPIA showed that *HDAC1* expression was up-regulated in DLBCL tissues (normal (N): $n = 337$; tumor (T): $n = 47$). (c,d) HDAC1 protein levels in three DLBCL samples ($n = 3$) and three normal samples ($n = 3$). (e) *HDAC1* expression in DLBCL cell lines, including OCI-LY-7 and SU-DHL-8, was assessed by RT-qPCR assay ($n = 3$). *$p < 0.05$, **$p < 0.01$, ***$p < 0.001$, ****$p < 0.0001$, compared with normal or GM12878 group. Abbreviations: DLBCL, Diffuse large B-cell lymphoma; HDAC1, Histone deacetylase 1; RT-qPCR, Real-time quantitative polymerase chain reaction; TCGA, The Cancer Genome Atlas; GEPIA, Gene Expression Profiling and Interactive Analyses; GAPDH, glyceraldehyde-3-phosphate dehydrogenase.

also remarkably elevated in DLBCL tissues (Fig. 1b) ($p < 0.05$). Western blotting was then adopted for analyzing the HDAC1 protein levels in three DLBCL samples and three normal controls. Results revealed that HDAC1 protein level was notably elevated in DLBCL tissues versus normal tissues (Fig. 1c,d) ($p < 0.05$). In addition, *HDAC1* expression was also detected in DLBCL cell lines, with the expression being higher in the DLBCL cells than in the GM12878 cells (Fig. 1e) ($p < 0.05$). Taken together, these findings point to the potential involvement of HDAC1 in DLBCL development.

HDAC1 Silencing Repressed DLBCL Cells' Proliferation and Glycolysis

Next, a lentivirus-mediated loss-of-function assay was adopted for knocking down *HDAC1* expression in DLBCL cells. RT-qPCR results illustrated that *HDAC1* expression was notably decreased after sh-*HDAC1* transfection, and sh-*HDAC1*#1 has the best gene silencing effect (Fig. 2a,b) ($p < 0.05$). Subsequently, both Western blotting and RT-qPCR results showed a consistent trend of *HDAC1* knockdown (Fig. 2c–f) ($p < 0.05$). Given that *HDAC1* was successfully knocked down, the sh-*HDAC1*#1 was selected for the follow-up experiments.

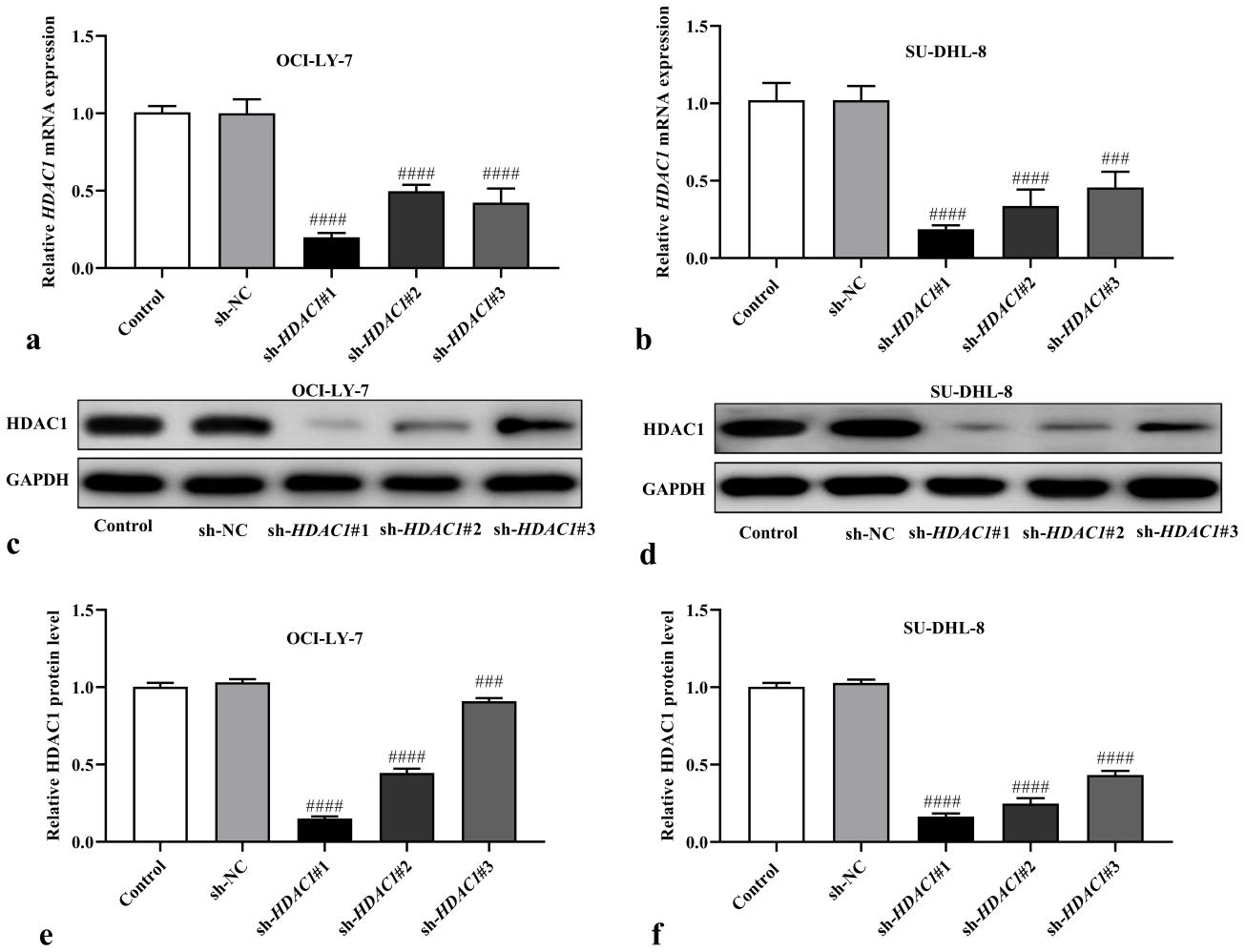

Fig. 2. HDAC1 expression was detected after sh-*HDAC1* transfection. (a,b) *HDAC1* mRNA expression was detected in cells after *HDAC1* knockdown ($n = 3$). (c–f) HDAC1 protein expression was detected in cells after *HDAC1* knockdown ($n = 3$). $^{###}p < 0.001$, $^{####}p < 0.0001$, compared with sh-NC. Abbreviations: HDAC1, Histone deacetylase 1; GAPDH, glyceraldehyde-3-phosphate dehydrogenase.

This research was conducted to investigate whether *HDAC1* knockdown affects the proliferation of the DLBCL cells, given that uncontrolled proliferation is a hallmark of malignant tumors. It was shown that inhibition of *HDAC1* expression repressed the viability of DLBCL cells (Fig. 3a,b) ($p < 0.05$). Meanwhile, EdU assay showed that *HDAC1* knockdown inhibited DLBCL cell proliferation (Fig. 3c–f) ($p < 0.05$). Additionally, according to flow cytometry results, *HDAC1* knockdown promoted cell apoptosis in DLBCL cells (Fig. 4a–d) ($p < 0.05$). *HDAC1* silencing also reduced the production of pyruvate, lactic acid, glucose consumption, and glycolysis-related protein expression in DLBCL cells (Fig. 5a–g) ($p < 0.05$). Therefore, *HDAC1* knockdown could inhibit the proliferation and glycolysis of DLBCL cells.

HDAC1 Silencing Inactivated PI3K/AKT/mTOR Pathway

The PI3K/AKT/mTOR pathway plays an indispensable role in the proliferation and metabolism of tumor cells. By analyzing expression of PI3K/AKT/mTOR pathway-related proteins in DLBCL cells following sh-*HDAC1*#1 transfection via Western blotting, we found that expression of p-PI3K, p-AKT and p-mTOR was reduced in the sh-*HDAC1*#1 group versus the sh-NC group in OCI-LY-7 and SU-DHL-8 cells (Fig. 6a–d) ($p < 0.05$). These findings indicate that *HDAC1* knockdown represses PI3K/AKT/mTOR pathway.

HDAC1 Regulated Proliferation and Glycolysis of OCI-LY-7 Cells Through PI3K/AKT/mTOR Pathway

HDAC1 knockdown inhibited the proliferation and glycolysis of DLBCL cells. To further clarify whether the impact of *HDAC1* knockdown on the proliferation and glycolysis of DLBCL cells is related to the PI3K/AKT/mTOR signaling pathway, a rescue experiment was conducted by using 740Y-P. The results confirmed that inhibition of *HDAC1* knockdown on cell proliferation was partly reversed by the addition of 740Y-P (Fig. 7a–c) ($p < 0.05$). The addition of 740Y-P also improved

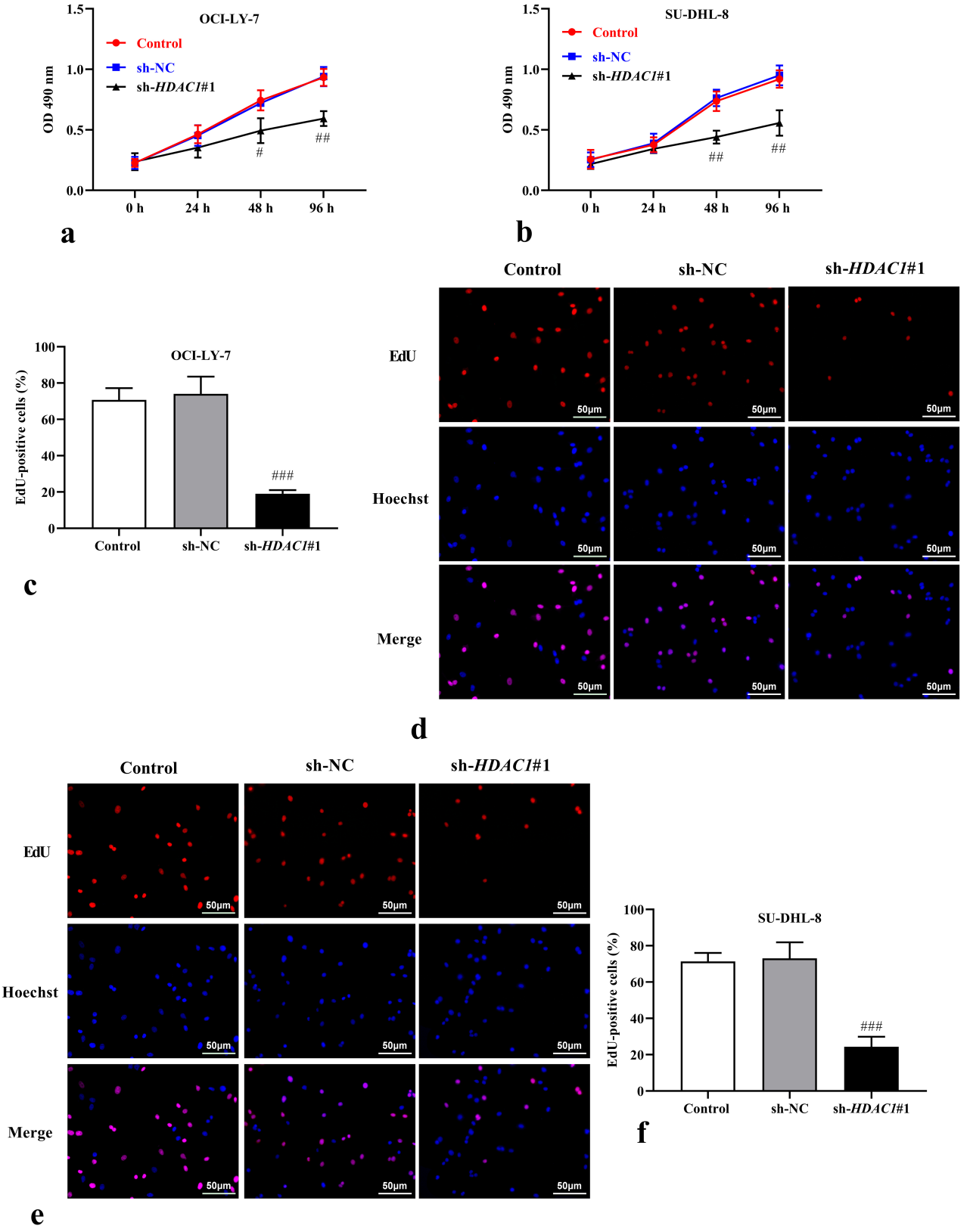

Fig. 3. *HDAC1* knockdown repressed the proliferation of DLBCL cells. (a,b) Viability of OCI-LY-7 and SU-DHL-8 cells with and without *HDAC1* knockdown as assessed using MTT assay (n = 3). (c–f) Effect of *HDAC1* knockdown on proliferation of OCI-LY-7 and SU-DHL-8 cells as measured by means of EdU assay (scale bar: 50 μm) (n = 3). $^{\#}p < 0.05$, $^{\#\#}p < 0.01$, $^{\#\#\#}p < 0.001$, compared with sh-NC. Abbreviations: DLBCL, Diffuse large B-cell lymphoma; HDAC1, Histone deacetylase 1; MTT, 3-(4,5)-dimethylthiahiazo (-z-y1)-3,5-di-phenytetrazoliumromide; EdU, 5-Ethynyl-2′-deoxyuridine.

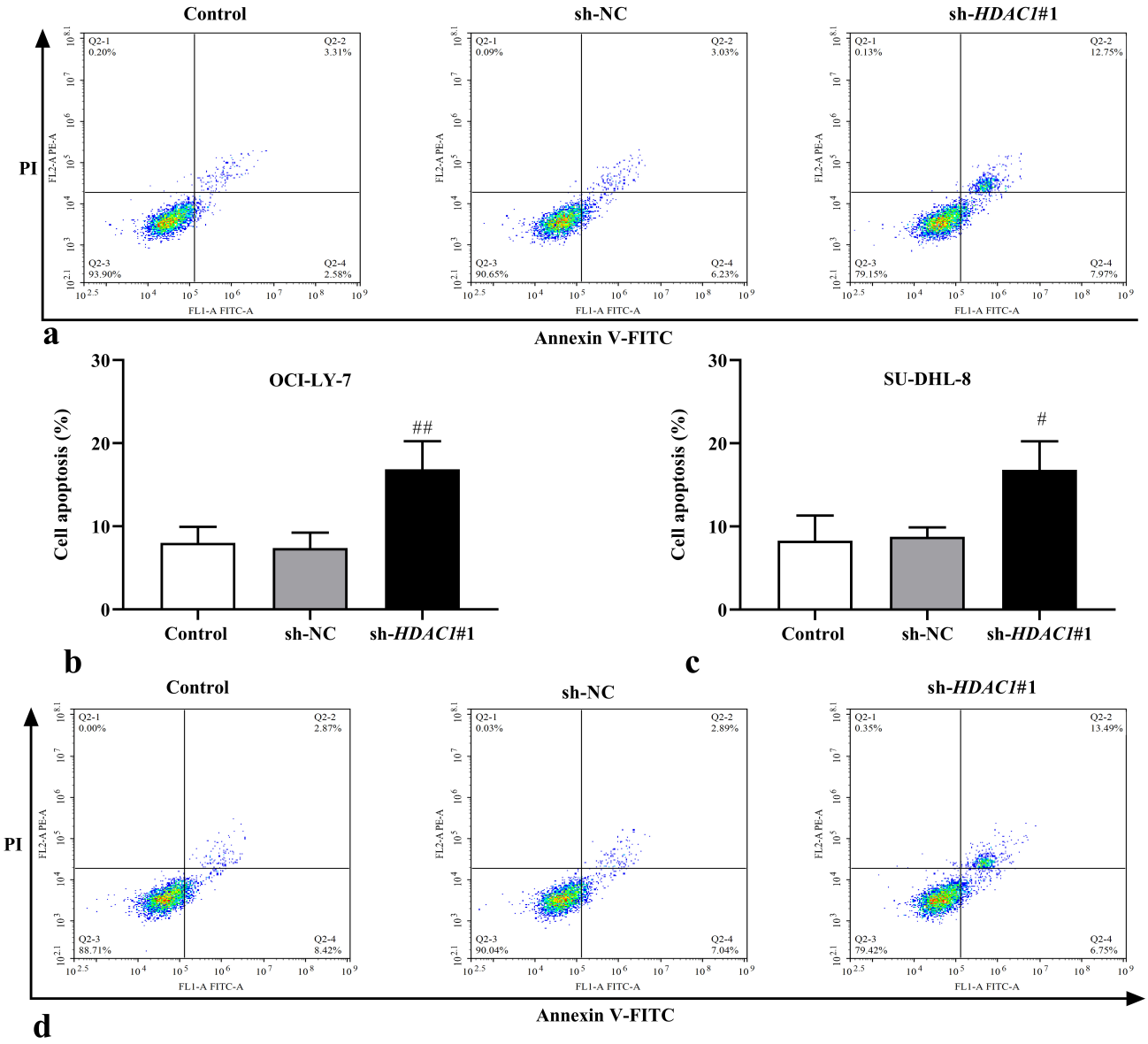

Fig. 4. *HDAC1* knockdown promoted apoptosis of DLBCL cells. (a–d) The effect of *HDAC1* knockdown on the apoptosis of OCI-LY-7 and SU-DHL-8 cells was measured using a flow cytometry assay ($n = 3$). $^{\#}p < 0.05$, $^{\#\#}p < 0.01$, compared with sh-NC. Abbreviations: DLBCL, Diffuse large B-cell lymphoma; HDAC1, Histone deacetylase 1.

cell apoptosis after *HDAC1* knockdown (Fig. 7d,e) ($p < 0.05$). In addition, the inhibiting effect on the glycolytic metabolism of sh-*HDAC1*#1+DMSO could be reversed by sh-*HDAC1*#1+740Y-P in cells (Fig. 8) ($p < 0.05$). These findings highlight that HDAC1 regulates the proliferation and glycolysis of DLBCL cells through the PI3K/AKT/mTOR pathway.

HDAC1 Knockdown Suppressed the Tumor Growth of DLBCL

In order to further verify the effect of HDAC1 expression level on tumor growth, OCI-LY-7 cells transfected with sh-*HDAC1*#1 were injected into mice to establish xenograft tumor model. HDAC1 level was decreased in the sh-*HDAC1*#1 group versus the sh-NC group (Fig. 9a–c) ($p < 0.05$). Injection of sh-*HDAC1*#1 significantly suppressed tumor volume (Fig. 9d,e) ($p < 0.05$). Moreover, tumor weight in the sh-*HDAC1*#1 group was decreased versus the sh-NC group (Fig. 9f) ($p < 0.05$). Based on the immunohistochemical staining results, *HDAC1* down-regulation significantly inhibited the HDAC1, Ki-67, and c-myc protein expression in mice (Fig. 10a–f) ($p < 0.05$), indicating that HDAC1 contributed to tumor growth of DLBCL *in vivo*.

Discussion

With existing therapies, approximately 40% of DLBCL patients can achieve sustained remission, but a significant proportion still face a prolonged clinical course

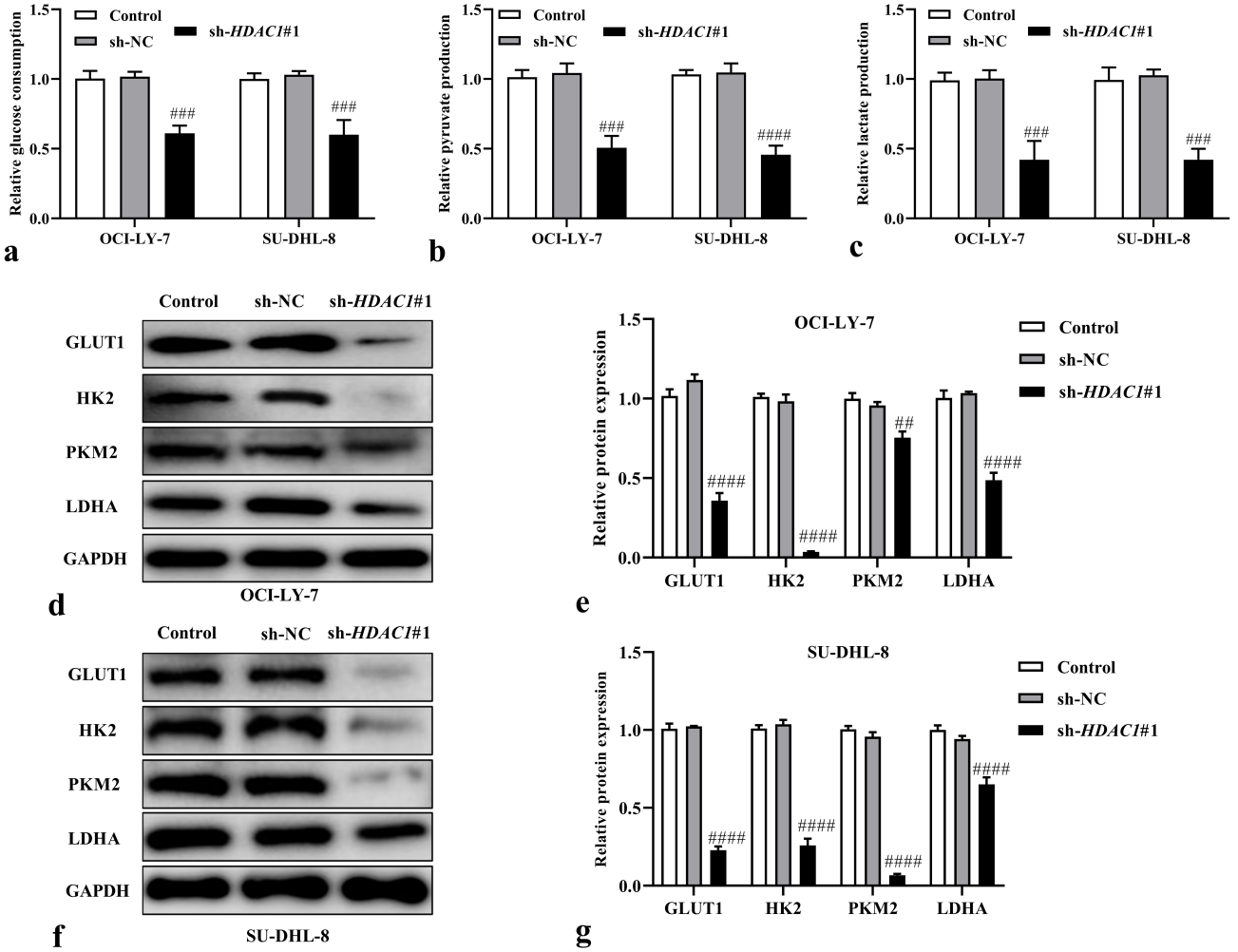

Fig. 5. *HDAC1* knockdown repressed glycolysis of DLBCL cells. (a–g) The effect of *HDAC1* knockdown on glucose consumption, pyruvate production, lactate production, and glycolysis-related protein expression in OCI-LY-7 and SU-DHL-8 cells (n = 3). $^{\#\#}p < 0.01$, $^{\#\#\#}p < 0.001$, $^{\#\#\#\#}p < 0.0001$, compared with sh-NC. Abbreviations: DLBCL, Diffuse large B-cell lymphoma; HDAC1, Histone deacetylase 1; GLUT1, Glucose transporter type 1; HK2, Hexokinase 2; PKM2, Pyruvate kinase muscle isoform 2; LDHA, Lactate dehydrogenase A; GAPDH, glyceraldehyde-3-phosphate dehydrogenase.

and unfavorable prognosis [30]. Therefore, this warrants the continued search for new biomolecular markers and therapeutic targets. The present study demonstrated that HDAC1 knockdown repressed DLBCL proliferation and aerobic glycolysis through the PI3K/AKT/mTOR pathway topic which has rarely been discussed. This study also further explores the role of HDAC1 during the development of DLBCL, providing new therapeutic ideas and insights for the treatment of DLBCL. This also contributes to a deeper understanding of the regulatory networks and mechanisms underlying DLBCL development, facilitating the translation of fundamental research into clinically relevant molecular markers and potential therapeutic targets. However, the precise mechanisms and their clinical application still require further investigation and validation.

HDAC is an important epigenetic regulator of tumors. Increased HDAC activity leads to silencing of tumor suppressor genes, resulting in abnormal growth of lymphoma [31]. Marquard *et al.* [32] reported higher expression of HDAC1, HDAC2 and HDAC6 in tumor tissues of DLBCL patients compared to lymphatic tissues of normal controls. Another study found that 89.7% of DLBCL patients were HDAC1-positive [33]. Notably, a previous study confirmed that HDAC1 and HDAC2 modulated B cell proliferation and apoptosis [34]. However, studies reporting the direct role of HDAC1 in DLBCL cell proliferation and glycolysis remain scarce. Ye [35] found that patients with high HDAC1 expression exhibited significantly poorer overall survival and progression-free survival compared to those with low expression, and that VPA (a selective HDAC inhibitor) could inhibit the growth and induce apoptosis of DLBCL cells with high HDAC1 expression. Min *et al.* [33] found that the proliferation index was correlated with HDAC1 expression level in cases of DLBCL. In the cur-

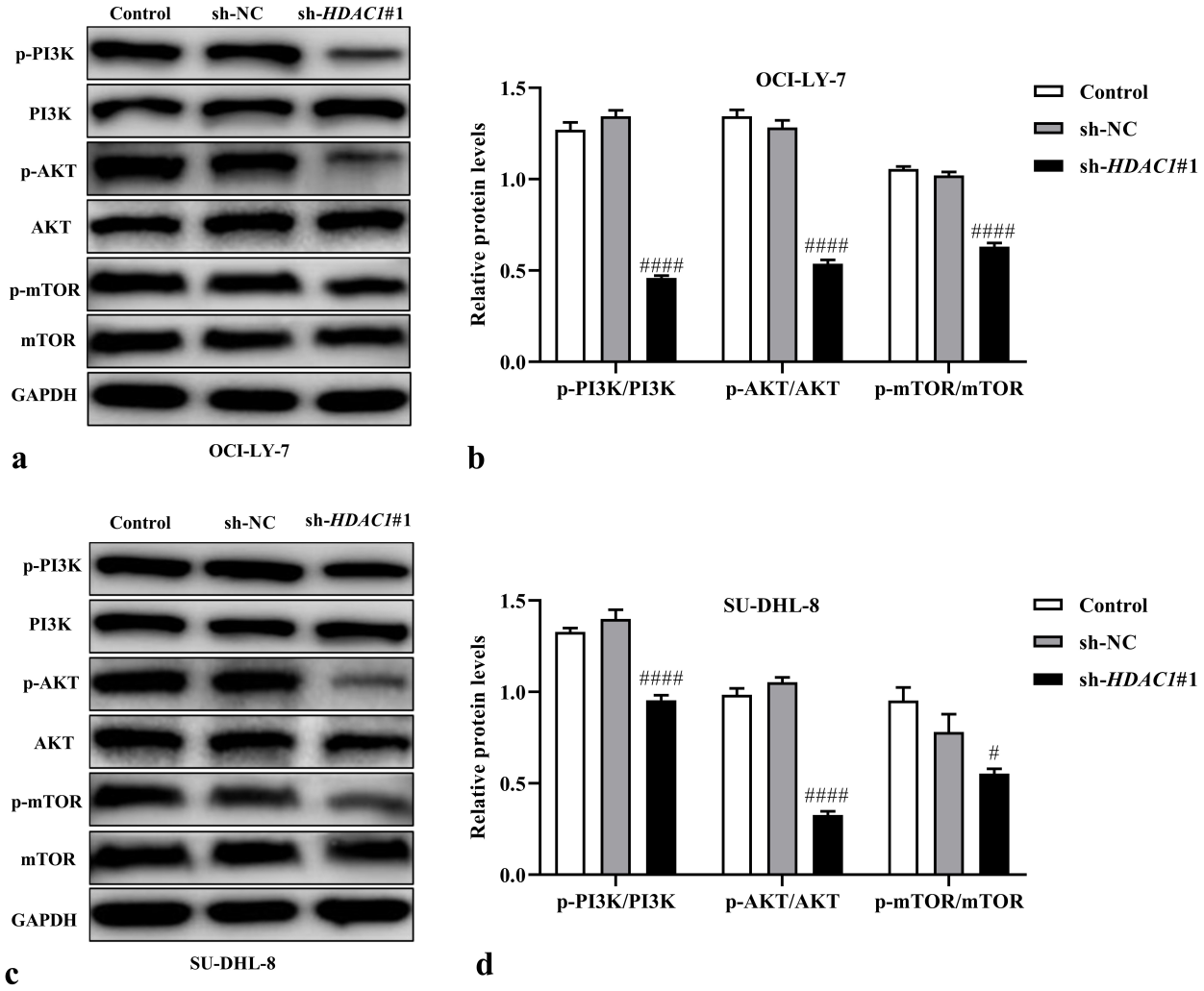

Fig. 6. *HDAC1* knockdown inactivated PI3K/AKT/mTOR pathway. (a–d) The expression of phosphorylated PI3K, AKT and mTOR in cells following sh-*HDAC1*#1 transfection, as measured using Western blotting ($n = 3$). $^{\#}p < 0.05$, $^{\#\#\#\#}p < 0.0001$, compared with sh-NC. Abbreviations: HDAC1, Histone deacetylase 1; PI3K, Phosphatidylinositol 3-kinase; AKT, protein kinase B; mTOR, mammalian target of rapamycin; GAPDH, glyceraldehyde-3-phosphate dehydrogenase.

rent research, we also found that HDAC1 knockdown suppressed DLBCL cell proliferation and promoted apoptosis. Moreover, HDAC1 knockdown repressed tumor growth of DLBCL *in vivo*. Multiple studies have shown that HDAC1 also plays a critical role in the glycolysis process of malignant tumors. HDAC1 has been found to promote glycolysis in GC progression [19], whereas in endometrial cancer, HDAC1 facilitates aerobic glycolysis and growth [26]. A published bioinformatics analysis revealed that the glioblastoma tissues with high HDAC1 levels exhibited remarkable expression of cancer markers, including those related to glycolysis [16]. This study found that HDAC1 silencing reduced the production of pyruvate, lactic acid, glucose consumption, and expression of glycolysis-related proteins in DLBCL cells. This indicates that HDAC1 plays a crucial role in regulating the glucose metabolism and proliferation of DLBCL cells.

The PI3K/AKT/mTOR pathway plays a crucial role in cell proliferation, survival, metabolism, and metastasis, and has been found to be abnormally activated in many cancer types [36]. It has been reported that HDAC1 promoted the malignant development of glioblastoma through the MEK/ERK and PI3K/AKT pathways [27]. As the main signal transduction pathway in tumor progression, the PI3K/AKT/mTOR pathway has been reported to be involved in the regulation of tumor growth and glycolysis of several cancer types [37–39]. A study found that pretreatment with either PI3K/AKT inhibitor or mTOR inhibitor aggravated the effects of KLK10 on colorectal cancer cell growth and glucose metabolism [40]. Moreover, andrographolide inhibited glycolysis via suppressing the PI3K/AKT/mTOR pathway, thereby enhancing the radiosensitivity of colorectal cancer [41]. Notably, the PI3K/AKT/mTOR pathway was abnormally activated in primary lymphoma of the central nervous system, con-

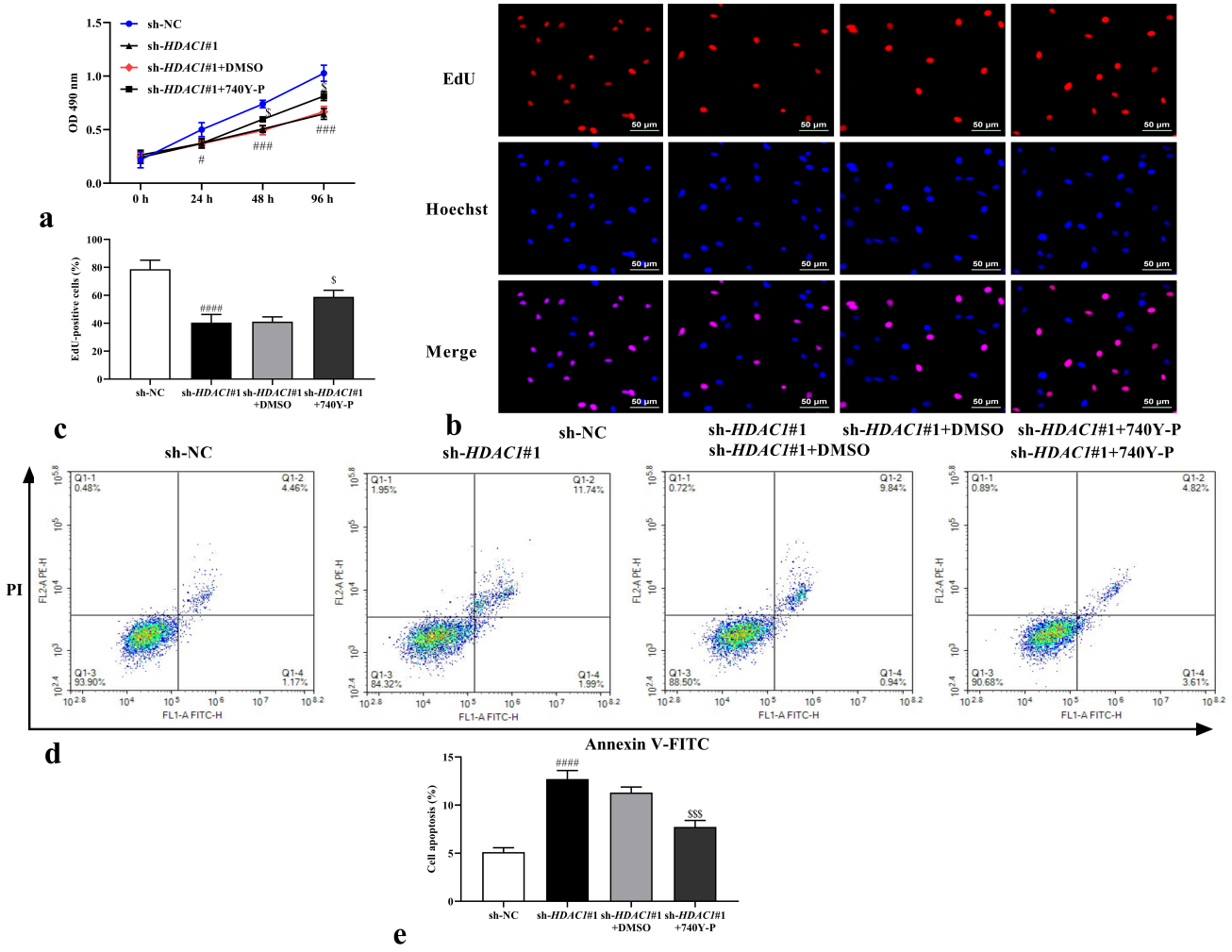

Fig. 7. 740Y-P reversed the inhibitory effect of *HDAC1* knockdown on the proliferation of OCI-LY-7 cells. (a–c) Evaluations of proliferative capacity of OCI-LY-7 cells treated with *HDAC1* knockdown and 740Y-P by means of MTT and EdU assays (scale bar: 50 μm) ($n = 3$). (d,e) Flow cytometric evaluations of the apoptosis of OCI-LY-7 cells treated with *HDAC1* knockdown and 740Y-P ($n = 3$). $^{\#}p < 0.05$, $^{\#\#\#}p < 0.001$, $^{\#\#\#\#}p < 0.0001$, compared with sh-NC. $^{\$}p < 0.05$, $^{\$\$\$}p < 0.001$, compared with sh-HDAC1#1+DMSO. Abbreviations: HDAC1, Histone deacetylase 1; MTT, 3-(4,5)-dimethylthiahiazo (-z-y1)-3,5-di-phenytetrazoliumromide; EdU, 5-Ethynyl-2′-deoxyuridine; DMSO, dimethyl sulfoxide.

tributing to an unfavorable prognosis [42]. Moreover, ROR1 knockdown notably inhibited the phosphorylation of PI3K, AKT and mTOR, but PI3K, AKT and mTOR protein levels in DLBCL cells were not significantly different between the ROR1 knockdown group and the control group [43]. However, whether HDAC1 affects cell proliferation and glycolysis in DLBCL through the PI3K/AKT/mTOR pathway remains unclear. Our results revealed that HDAC1 knockdown was able to inhibit phosphorylation of PI3K, AKT, and mTOR proteins in cells. Moreover, the inhibitory effect of HDAC1 knockdown on cell proliferation and glycolysis could be reversed by 740Y-P. Therefore, our findings suggest that HDAC1 plays a critical role in DLBCL development by promoting tumor cell proliferation and glycolysis, while inhibiting apoptosis, through activation of the PI3K/AKT/mTOR pathway.

Based on the heterogeneity of tumor energy metabolism, DLBCL can be classified into oxidative phosphorylation (OxPhos) and non-oxidative phosphorylation (non-OxPhos) subtypes [44]. In the OxPhos subtype of DLBCL, genes related to mitochondrial oxidative phosphorylation are upregulated, and cells show increased dependence on fatty acid β-oxidation (FAO) for energy production. In contrast, the non-OxPhos subtype exhibits abnormally elevated glycolytic activity [45,46]. Approximately 60% of the total energy of DLBCL cells is derived from aerobic glycolysis [47]. Targeting the energy metabolism pathways involved in DLBCL may provide new insights for improving treatment strategies and prognostic assessment. Metabolic heterogeneity among DLBCL subtypes highlights the potential for individualized, precision treatment. Identifying differences in energy

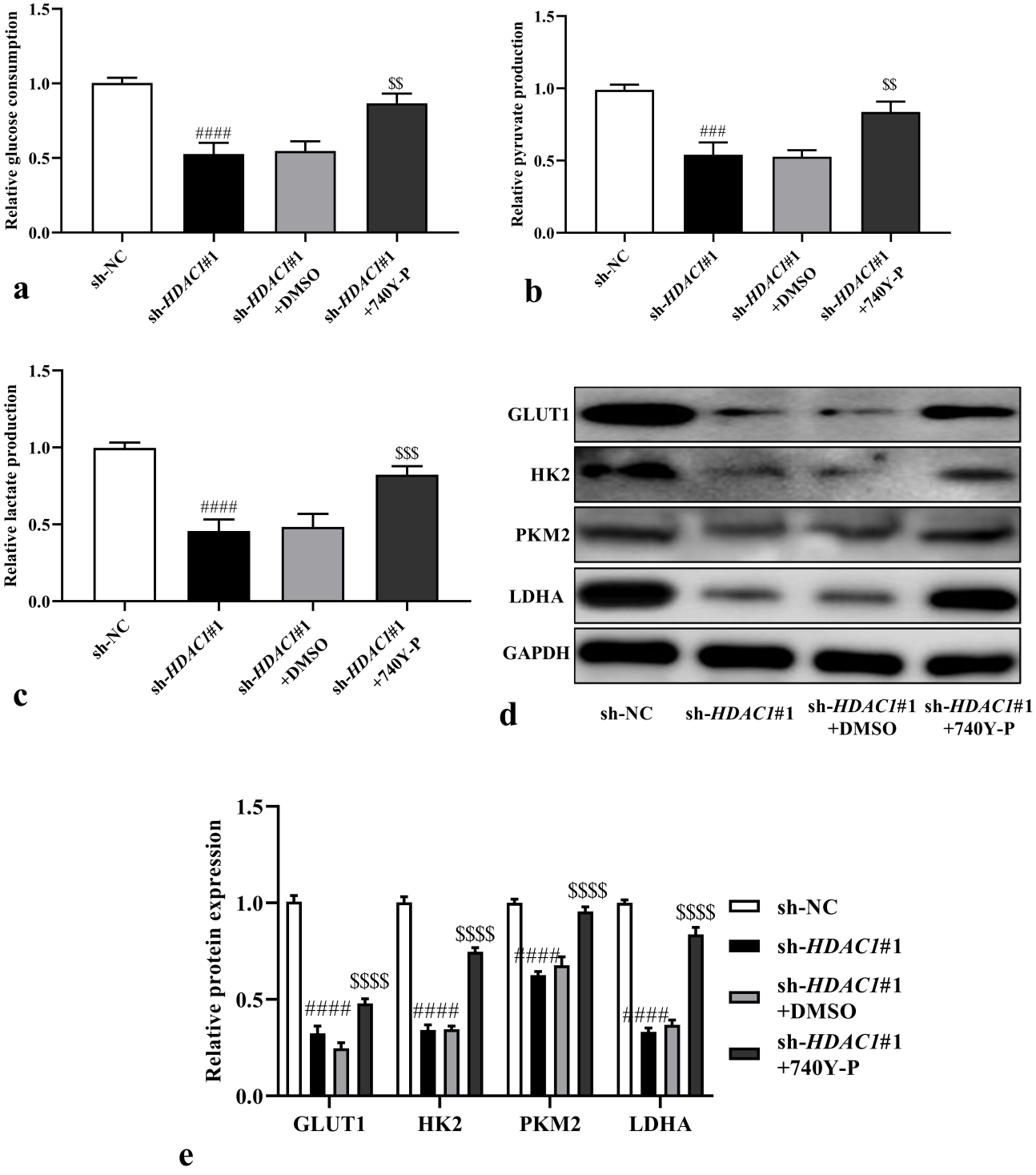

Fig. 8. 740Y-P reversed inhibitory effect of *HDAC1* knockdown on the glycolysis of OCI-LY-7 cells. (a–c) Effect of 740Y-P on glucose consumption, pyruvate production, and lactate production of OCI-LY-7 cells treated with *HDAC1* knockdown ($n = 3$). (d,e) Effect of 740Y-P on the expression of glycolysis-related proteins in OCI-LY-7 cells treated with *HDAC1* knockdown, as analyzed using Western blotting (d), and the corresponding quantitative measurements of the protein expression ($n = 3$). $^{\#\#\#}p < 0.001$, $^{\#\#\#\#}p < 0.0001$, compared with sh-NC. $^{\$\$}p < 0.01$, $^{\$\$\$}p < 0.001$, $^{\$\$\$\$}p < 0.0001$, compared with sh-*HDAC1*#1+DMSO. Abbreviations: HDAC1, Histone deacetylase 1; DMSO, dimethyl sulfoxide; GLUT1, Glucose transporter type 1; HK2, Hexokinase 2; PKM2, Pyruvate kinase muscle isoform 2; LDHA, Lactate dehydrogenase A; GAPDH, glyceraldehyde-3-phosphate dehydrogenase.

metabolism among different subtypes of DLBCL, as well as biomarkers and therapeutic targets for these subtypes, could open new avenues for the personalized treatment of DLBCL patients. Here, HDAC1 plays a certain regulatory

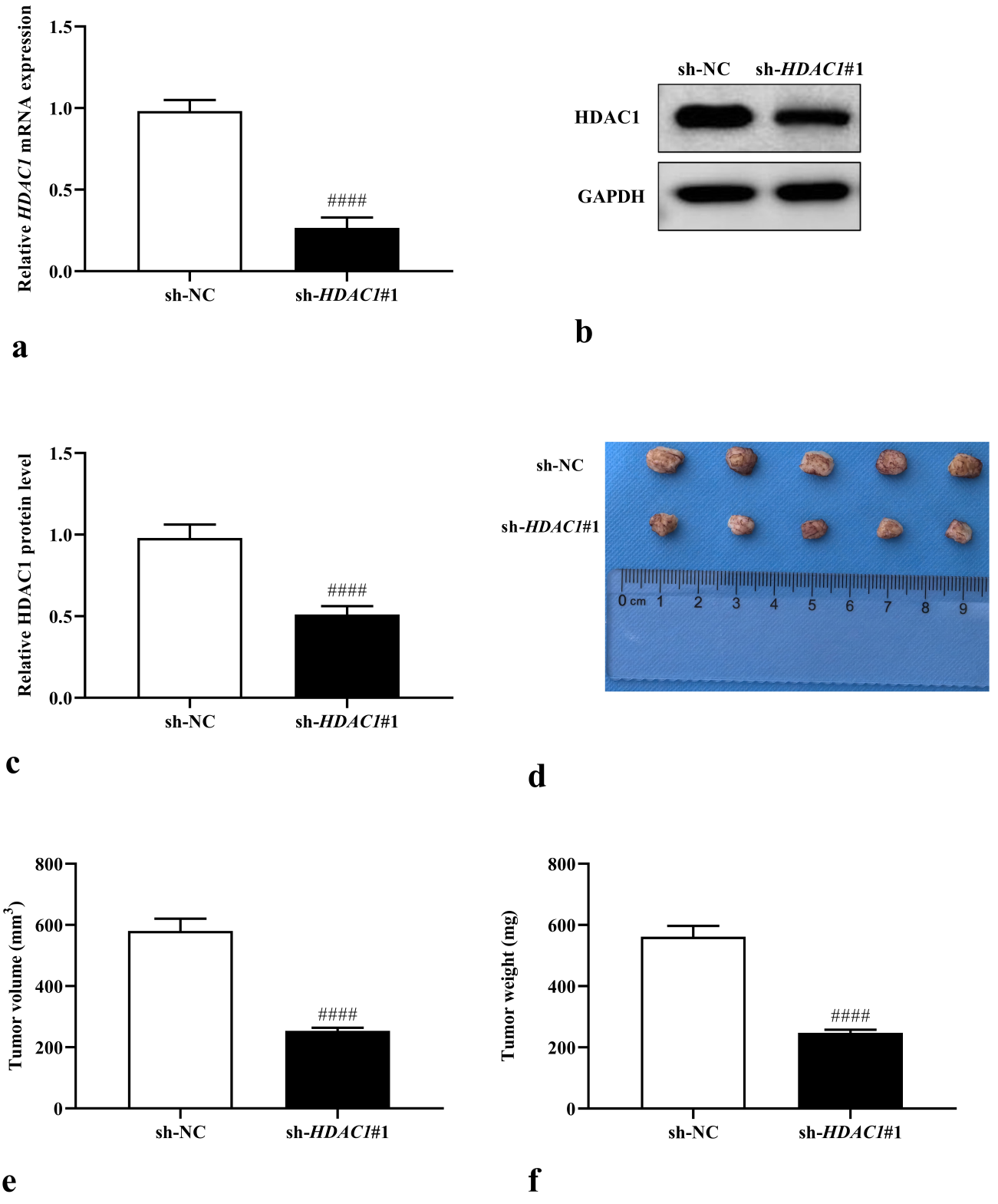

Fig. 9. *HDAC1* knockdown repressed tumor growth of DLBCL. (a–c) Expression of HDAC1 mRNA and protein in xenograft tumor model ($n = 5$). (d,e) Effect of sh-*HDAC1*#1 on tumor growth and volume in mice ($n = 5$). (f) Effect of sh-*HDAC1*#1 on tumor weight in mice ($n = 5$). $^{\#\#\#\#}p < 0.0001$, compared with sh-NC. Abbreviations: DLBCL, Diffuse large B-cell lymphoma; HDAC1, Histone deacetylase 1; GAPDH, glyceraldehyde-3-phosphate dehydrogenase.

role in the energy metabolism of DLBCL tumor cells by regulating the PI3K/AKT/mTOR pathway. With the in-depth study of tumor epigenetics, the role of HDAC inhibitors in tumor occurrence and development has in-

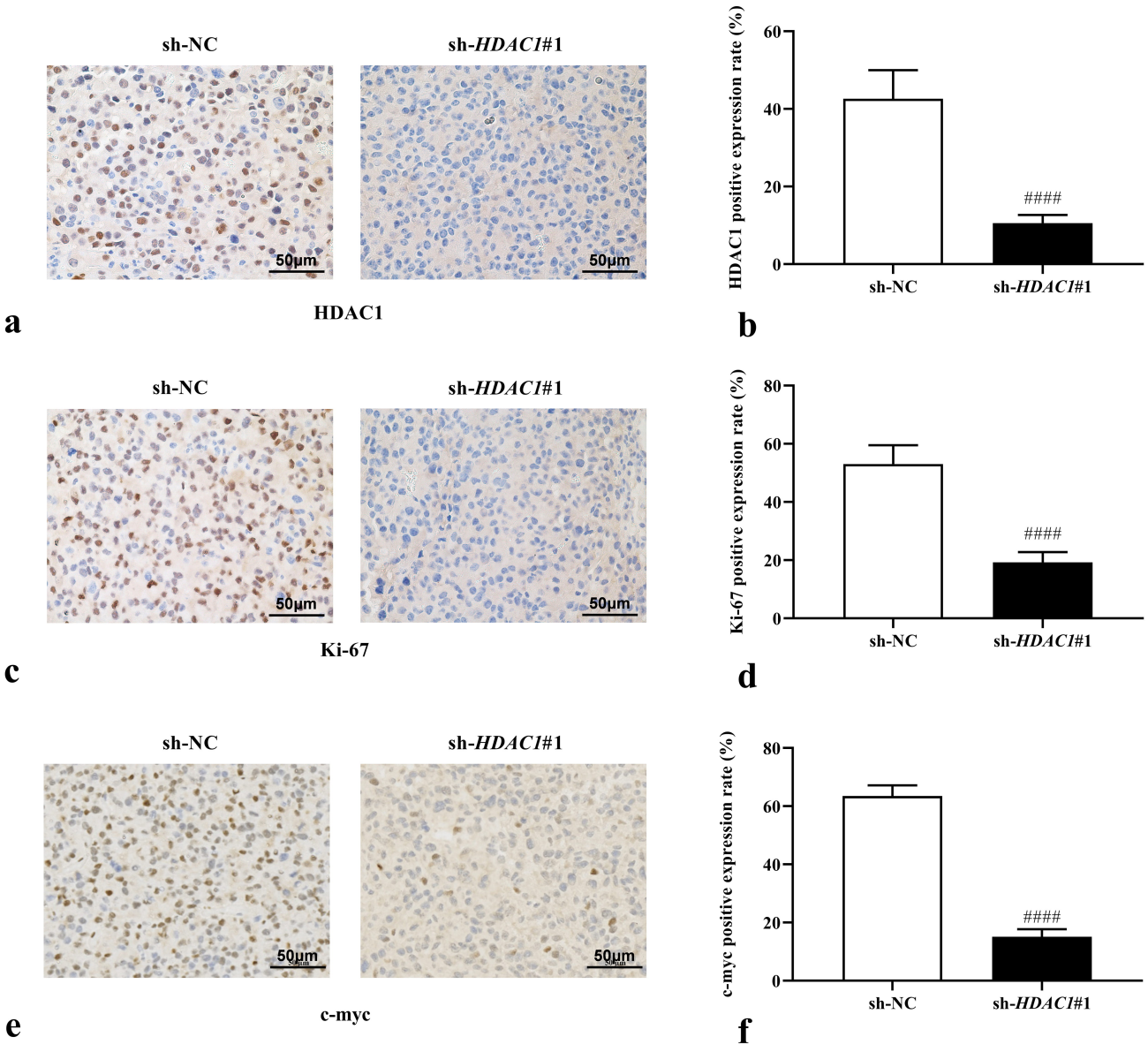

Fig. 10. Immunohistochemical detection and quantitative analysis of HDAC1 (a,b), Ki-67 (c,d), and c-myc expression (e,f) in mice tumor (n = 5). $^{####}p < 0.0001$, compared with sh-NC. Abbreviations: HDAC1, Histone deacetylase 1.

creasingly attracted the attention of researchers. Currently, HDAC inhibitors have been used in the treatment and clinical research of DLBCL [48–51]. Inhibitors targeting the PI3K/AKT/mTOR pathway have also shown promising progress in the clinical treatment of DLBCL [52,53]. Compared to single-agent treatments, combination therapies may offer superior clinical efficacy, highlighting their promising potential in clinical application. In light of this, gaining a deeper understanding of drugs and treatment methods related to HDAC1 and the PI3K/AKT/mTOR pathway may yield new insights for treating DLBCL and improving patient prognosis.

This study is not without limitations. Firstly, the present study utilized a relatively small-sized sample and limited subtypes of patients, necessitating a larger cohort to support our viewpoint. Additionally, only two cell lines were employed in the functional experiments; therefore, incorporating a broader range of cell line types in future studies is necessary to more accurately elucidate the function of HDAC1. Due to the less competent laboratory conditions and insufficient research funds, we were unable to further investigate the regulatory relationship between HDAC1 and the PI3K/AKT/mTOR pathway. Aside from the above-mentioned shortcomings, several research questions remain unanswered: For example, how does HDAC1 regulate PI3K/AKT/mTOR? Does HDAC1 directly bind to the regulatory regions of PI3K, AKT or mTOR genes? Does HDAC1 participate in other mechanisms related to the progression of DLBCL through the PI3K/AKT/mTOR pathway? In summary, the regulatory mechanisms underly-

ing DLBCL development remain incompletely understood, but they represent a key focus for our future investigations.

Conclusions

This study demonstrated that HDAC1 expression is markedly elevated in DLBCL tissues and cells. Knockdown of HDAC1 suppresses cell proliferation and glycolysis in DLBCL through the PI3K/AKT/mTOR pathway. These findings highlight the pivotal role of the HDAC1 in DLBCL development and provide a theoretical foundation for establishing HDAC1 as a promising therapeutic target in the development of novel treatment strategies for DLBCL.

Availability of Data and Materials

The datasets used and/or analyzed during the current study are available from the corresponding author on reasonable request.

Author Contributions

YZW and XJF conceived and designed the study and drafted the manuscript. YZW, YW, SSW, FRZ and XMY collected, analyzed and interpreted the data. All authors were involved in the drafting and critical revision of the manuscript. All authors have read and approved the final manuscript. All authors have participated sufficiently in the work and agreed to be accountable for all aspects of the work.

Ethics Approval and Consent to Participate

This research complies with the requirements of the Declaration of Helsinki. This study was approved by the ethics committee of Yantaishan Hospital (approval no. 2024047). Informed consent was obtained from all patients.

Acknowledgment

Not applicable.

Funding

This research received no external funding.

Conflict of Interest

The authors declare no conflict of interest.

References

[1] Coiffier B. Current strategies for the treatment of diffuse large B cell lymphoma. Current Opinion in Hematology. 2005; 12: 259–265. https://doi.org/10.1097/01.moh.0000168519.98990.94.

[2] Smith A, Roman E, Howell D, Jones R, Patmore R, Jack A, *et al*. The Haematological Malignancy Research Network (HMRN): a new information strategy for population based epidemiology and health service research. British Journal of Haematology. 2010; 148: 739–753. https://doi.org/10.1111/j.1365-2141.2009.08010.x.

[3] Johnson NA, Slack GW, Savage KJ, Connors JM, Ben-Neriah S, Rogic S, *et al*. Concurrent expression of MYC and BCL2 in diffuse large B-cell lymphoma treated with rituximab plus cyclophosphamide, doxorubicin, vincristine, and prednisone. Journal of Clinical Oncology. 2012; 30: 3452–3459. https://doi.org/10.1200/JCO.2011.41.0985.

[4] Oki Y, Ewer MS, Lenihan DJ, Fisch MJ, Hagemeister FB, Fanale M, *et al*. Pegylated liposomal doxorubicin replacing conventional doxorubicin in standard R-CHOP chemotherapy for elderly patients with diffuse large B-cell lymphoma: an open label, single arm, phase II trial. Clinical Lymphoma, Myeloma & Leukemia. 2015; 15: 152–158. https://doi.org/10.1016/j.clml.2014.09.001.

[5] Dobish KK, Wittorf KJ, Swenson SA, Bean DC, Gavile CM, Woods NT, *et al*. FBXO21 mediated degradation of p85α regulates proliferation and survival of acute myeloid leukemia. Leukemia. 2023; 37: 2197–2208. https://doi.org/10.1038/s41375-023-02020-w.

[6] Matsumoto S, Harada A, Seta M, Akita M, Gon H, Fukumoto T, *et al*. Wnt Signaling Stimulates Cooperation between GREB1 and HNF4α to Promote Proliferation in Hepatocellular Carcinoma. Cancer Research. 2023; 83: 2312–2327. https://doi.org/10.1158/0008-5472.CAN-22-3518.

[7] Feitelson MA, Arzumanyan A, Kulathinal RJ, Blain SW, Holcombe RF, Mahajna J, *et al*. Sustained proliferation in cancer: Mechanisms and novel therapeutic targets. Seminars in Cancer Biology. 2015; 35: S25–S54. https://doi.org/10.1016/j.semcancer.2015.02.006.

[8] Nguyen DD, Kim E, Le NT, Ding X, Jaiswal RK, Kostlan RJ, *et al*. Deficiency in mammalian STN1 promotes colon cancer development via inhibiting DNA repair. Science Advances. 2023; 9: eadd8023. https://doi.org/10.1126/sciadv.add8023.

[9] Hanahan D, Weinberg RA. Hallmarks of cancer: the next generation. Cell. 2011; 144: 646–674. https://doi.org/10.1016/j.cell.2011.02.013.

[10] Warburg O. On respiratory impairment in cancer cells. Science. 1956; 124: 269–270.

[11] WARBURG O. On the origin of cancer cells. Science. 1956; 123: 309–314. https://doi.org/10.1126/science.123.3191.309.

[12] Reinfeld BI, Rathmell WK, Kim TK, Rathmell JC. The therapeutic implications of immunosuppressive tumor aerobic glycolysis. Cellular & Molecular Immunology. 2022; 19: 46–58. https://doi.org/10.1038/s41423-021-00727-3.

[13] Sun J, Piao J, Li N, Yang Y, Kim KY, Lin Z. Valproic acid targets HDAC1/2 and HDAC1/PTEN/Akt signalling to inhibit cell proliferation via the induction of autophagy in gastric cancer. The FEBS Journal. 2020; 287: 2118–2133. https://doi.org/10.1111/febs.15122.

[14] He Z, Zhong Y, Hu H, Li F. ZFP64 Promotes Gallbladder Cancer Progression through Recruiting HDAC1 to Activate NOTCH1 Signaling Pathway. Cancers. 2023; 15: 4508. https://doi.org/10.3390/cancers15184508.

[15] Wang S, Cui Z, Zhu J, Zhou P, Cao X, Li X, *et al*. Colchicine inhibits the proliferation and promotes the apoptosis of papillary thyroid carcinoma cells likely due to the inhibitory effect on HDAC1. Biochemical and Biophysical Research Communications. 2023; 679: 129–138. https://doi.org/10.1016/j.bbrc.2023.09.006.

[16] Cheng Z, Li S, Yuan J, Li Y, Cheng S, Huang S, *et al*. HDAC1 mediates epithelial-mesenchymal transition and promotes cancer cell invasion in glioblastoma. Pathology, Research and Practice. 2023; 246: 154481. https://doi.org/10.1016/j.prp.2023.154481.

[17] Nagarajan S, Rao SV, Sutton J, Cheeseman D, Dunn S, Papachristou EK, *et al*. ARID1A influences HDAC1/BRD4 activity, intrinsic proliferative capacity and breast cancer treatment response. Nature Genetics. 2020; 52: 187–197. https://doi.org/10.1038/s41588-019-0541-5.

[18] Singh A, Gupta S, Sachan M. Epigenetic Biomarkers in the Management of Ovarian Cancer: Current Prospectives. Frontiers in Cell and Developmental Biology. 2019; 7: 182. https://doi.org/10.3389/fcell.2019.00182.

[19] Jiang Z, Yang H, Zhang X, Wang Z, Rong R, Wang X. Histone deacetylase-1 as a prognostic factor and mediator of gastric cancer progression by enhancing glycolysis. Human Pathology. 2019; 85: 194–201. https://doi.org/10.1016/j.humpath.2018.10.031.

[20] Abdollahi S, Dehghanian SZ, Hung LY, Yang SJ, Chen DP, Medeiros LJ, *et al*. Deciphering genes associated with diffuse large B-cell lymphoma with lymphomatous effusions: A mutational accumulation scoring approach. Biomarker Research. 2021; 9: 74. https://doi.org/10.1186/s40364-021-00330-8.

[21] Murai T, Matsuda S. Targeting the PI3K-Akt-mTOR signaling pathway involved in vasculogenic mimicry promoted by cancer stem cells. American Journal of Cancer Research. 2023; 13: 5039–5046.

[22] Vujičić Žagar A, Scapozza L, Vadas O. Design and purification of active truncated phosphoinositide 3-kinase gamma protein constructs for structural studies. Protein Expression and Purification. 2017; 135: 1–7. https://doi.org/10.1016/j.pep.2017.04.011.

[23] Jiang BH, Liu LZ. PI3K/PTEN signaling in tumorigenesis and angiogenesis. Biochimica et Biophysica Acta. 2008; 1784: 150–158. https://doi.org/10.1016/j.bbapap.2007.09.008.

[24] Cao J, Cao R, Liu Y, Dai T. CPNE1 mediates glycolysis and metastasis of breast cancer through activation of PI3K/AKT/HIF-1α signaling. Pathology, Research and Practice. 2023; 248: 154634. https://doi.org/10.1016/j.prp.2023.154634.

[25] Li Z, Jiang Y, Liu J, Fu H, Yang Q, Song W, *et al*. Exosomes from PYCR1 knockdown bone marrow mesenchymal stem inhibits aerobic glycolysis and the growth of bladder cancer cells via regulation of the EGFR/PI3K/AKT pathway. International Journal of Oncology. 2023; 63: 84. https://doi.org/10.3892/ijo.2023.5532.

[26] Wu Q, Zhang W, Liu Y, Huang Y, Wu H, Ma C. Histone deacetylase 1 facilitates aerobic glycolysis and growth of endometrial cancer. Oncology Letters. 2021; 22: 721. https://doi.org/10.3892/ol.2021.12982.

[27] Li S, Chen X, Mao L, Zahid KR, Wen J, Zhang L, *et al*. Histone deacetylase 1 promotes glioblastoma cell proliferation and invasion via activation of PI3K/AKT and MEK/ERK signaling pathways. Brain Research. 2018; 1692: 154–162. https://doi.org/10.1016/j.brainres.2018.05.023.

[28] Ma S, Liu T, Xu L, Wang Y, Zhou J, Huang T, *et al*. Histone deacetylases inhibitor MS-275 suppresses human esophageal squamous cell carcinoma cell growth and progression via the PI3K/Akt/mTOR pathway. Journal of Cellular Physiology. 2019; 234: 22400–22410. https://doi.org/10.1002/jcp.28805.

[29] Chen L, Zhuo D, Yuan H. Circ_100395 impedes malignancy and glycolysis in papillary thyroid cancer: Involvement of PI3K/AKT/mTOR signaling pathway. Immunology Letters. 2022; 246: 10–17. https://doi.org/10.1016/j.imlet.2022.04.004.

[30] Feng Q, Hu K, Hu H, Lu Y, Zhang H, Wang G, *et al*. Berberine derivative DCZ0358 induce oxidative damage by ROS-mediated JNK signaling in DLBCL cells. International Immunopharmacology. 2023; 125: 111139. https://doi.org/10.1016/j.intimp.2023.111139.

[31] Batlevi CL, Crump M, Andreadis C, Rizzieri D, Assouline SE, Fox S, *et al*. A phase 2 study of mocetinostat, a histone deacetylase inhibitor, in relapsed or refractory lymphoma. British Journal of Haematology. 2017; 178: 434–441. https://doi.org/10.1111/bjh.14698.

[32] Marquard L, Poulsen CB, Gjerdrum LM, de Nully Brown P, Christensen IJ, Jensen PB, *et al*. Histone deacetylase 1, 2, 6 and acetylated histone H4 in B- and T-cell lymphomas. Histopathology. 2009; 54: 688–698. https://doi.org/10.1111/j.1365-2559.2009.03290.x.

[33] Min SK, Koh YH, Park Y, Kim HJ, Seo J, Park HR, *et al*. Expression of HAT1 and HDAC1, 2, 3 in Diffuse Large B-Cell Lymphomas, Peripheral T-Cell Lymphomas, and NK/T-Cell Lymphomas. Korean Journal of Pathology. 2012; 46: 142–150. https://doi.org/10.4132/KoreanJPathol.2012.46.2.142.

[34] Yamaguchi T, Cubizolles F, Zhang Y, Reichert N, Kohler H, Seiser C, *et al*. Histone deacetylases 1 and 2 act in concert to promote the G1-to-S progression. Genes & Development. 2010; 24: 455–469. https://doi.org/10.1101/gad.552310.

[35] Ye JX. The expression of histone deacetylases 1 in DLBCL and its prognostic significance [master's dissertation]. Zhejiang University. 2018.

[36] Glaviano A, Foo ASC, Lam HY, Yap KCH, Jacot W, Jones RH, *et al*. PI3K/AKT/mTOR signaling transduction pathway and targeted therapies in cancer. Molecular Cancer. 2023; 22: 138. https://doi.org/10.1186/s12943-023-01827-6.

[37] Wang K, Li J, Zhou B. KIAA0101 knockdown inhibits glioma progression and glycolysis by inactivating the PI3K/AKT/mTOR pathway. Metabolic Brain Disease. 2022; 37: 489–499. https://doi.org/10.1007/s11011-021-00863-9.

[38] Li Z, Jin Q, Sun Y. LINC00941 promoted in vitro progression and glycolysis of laryngocarcinoma by upregulating PKM via activating the PI3K/AKT/mTOR signaling pathway. Journal of Clinical Laboratory Analysis. 2022; 36: e24406. https://doi.org/10.1002/jcla.24406.

[39] Zhang Y, Wu Y, Su X. PLOD1 promotes cell growth and aerobic glycolysis by regulating the SOX9/PI3K/Akt/mTOR signaling pathway in gastric cancer. Frontiers in Bioscience-Landmark. 2021; 26: 322–334. https://doi.org/10.52586/4946.

[40] Wei H, Dong C, Shen Z. Kallikrein-related peptidase (KLK10) cessation blunts colorectal cancer cell growth and glucose metabolism by regulating the PI3K/Akt/mTOR pathway. Neoplasma. 2020; 67: 889–897. https://doi.org/10.4149/neo_2020_190814N758.

[41] Li X, Tian R, Liu L, Wang L, He D, Cao K, *et al*. Andrographolide enhanced radiosensitivity by downregulating glycolysis via the inhibition of the PI3K-Akt-mTOR signaling pathway in HCT116 colorectal cancer cells. The Journal of International Medical Research. 2020; 48: 300060520946169. https://doi.org/10.1177/0300060520946169.

[42] Zhang X, Wu Y, Sun X, Cui Q, Bai X, Dong G, *et al*. The PI3K/AKT/mTOR signaling pathway is aberrantly activated in primary central nervous system lymphoma and correlated with a poor prognosis. BMC Cancer. 2022; 22: 190. https://doi.org/10.1186/s12885-022-09275-z.

[43] Mao Y, Xu L, Wang J, Zhang L, Hou N, Xu J, *et al*. ROR1 associates unfavorable prognosis and promotes lymphoma growth in DLBCL by affecting PI3K/Akt/mTOR signaling pathway. BioFactors. 2019; 45: 416–426. https://doi.org/10.1002/biof.1498.

[44] Dawiec P, Leszczenko P, Nowakowska AM, Laskowska P, Szydłowski M, Juszczyński P, *et al*. Automatic subtyping of Diffuse Large B-cell Lymphomas (DLBCL): Raman-based genetic and metabolic classification. Spectrochimica Acta. Part A, Molecular and Biomolecular Spectroscopy. 2024; 309: 123795. https://doi.org/10.1016/j.saa.2023.123795.

[45] Caro P, Kishan AU, Norberg E, Stanley IA, Chapuy B, Ficarro SB, *et al*. Metabolic signatures uncover distinct targets in molec-

ular subsets of diffuse large B cell lymphoma. Cancer Cell. 2012; 22: 547–560. https://doi.org/10.1016/j.ccr.2012.08.014.

[46] Jiang D, Mo Q, Sun X, Wang X, Dong M, Zhang G, *et al*. Pyruvate dehydrogenase kinase 4-mediated metabolic reprogramming is involved in rituximab resistance in diffuse large B-cell lymphoma by affecting the expression of MS4A1/CD20. Cancer Science. 2021; 112: 3585–3597. https://doi.org/10.1111/cas.15055.

[47] Gong X, Gong YQ, Ding LY, Lei LZ, Zhou R. Energy metabolism classification and research progress of diffuse large B cell lymphoma. Chinese Journal of Pathology. 2019; 48: 63–66. https://doi.org/10.3760/cma.j.issn.0529-5807.2019.01.017. (In Chinese)

[48] Wang M, Fang X, Wang X. Emerging role of histone deacetylase inhibitors in the treatment of diffuse large B-cell lymphoma. Leukemia & Lymphoma. 2020; 61: 763–775. https://doi.org/10.1080/10428194.2019.1691194.

[49] Kim SJ, Kim UJ, Yoo HY, Choi YJ, Kang KW. Anti-Cancer Effects of CKD-581, a Potent Histone Deacetylase Inhibitor against Diffuse Large B-Cell Lymphoma. International Journal of Molecular Sciences. 2020; 21: 4377. https://doi.org/10.3390/ijms21124377.

[50] Dupire S, Coiffier B. Targeted treatment and new agents in diffuse large B cell lymphoma. International Journal of Hematology. 2010; 92: 12–24. https://doi.org/10.1007/s12185-010-0609-6.

[51] Wu C, Song Q, Gao S, Wu S. Targeting HDACs for diffuse large B-cell lymphoma therapy. Scientific Reports. 2024; 14: 289. https://doi.org/10.1038/s41598-023-50956-x.

[52] Xu ZZ, Xia ZG, Wang AH, Wang WF, Liu ZY, Chen LY, *et al*. Activation of the PI3K/AKT/mTOR pathway in diffuse large B cell lymphoma: clinical significance and inhibitory effect of rituximab. Annals of Hematology. 2013; 92: 1351–1358. https://doi.org/10.1007/s00277-013-1770-9.

[53] Majchrzak A, Witkowska M, Smolewski P. Inhibition of the PI3K/Akt/mTOR signaling pathway in diffuse large B-cell lymphoma: current knowledge and clinical significance. Molecules. 2014; 19: 14304–14315. https://doi.org/10.3390/molecules190914304.